Research Article

Thermal degradation kinetics of total anthocyanins in açaí pulp and transient processing simulations

Luís Marangoni Júnior[1] · Gustavo De Bastiani[1] · Roniérik Pioli Vieira[2] · Carlos Alberto Rodrigues Anjos[1]

Received: 9 January 2020 / Accepted: 25 February 2020 / Published online: 2 March 2020

Abstract
The aim of this study was to investigate the thermal degradation of açaí pulp anthocyanins in experimental level and to simulate its degradation in a tubular pasteurizer starting from the transient regime. Thermal degradation was experimentally performed at 60, 70, 80, and 90 °C, in which samples were collected throughout 90 min. Anthocyanin concentration was determined using the differential pH method. The first-order kinetic model with low activation energy (42.8 kJ mol^{-1}) and the thermodynamic parameters obtained ($\Delta H > 0$, $\Delta G > 0$, and $\Delta S < 0$) confirmed the high thermal stability of anthocyanin in açaí pulp. For the simulations, the mass and energy balances took into consideration a transient regime and also variation of anthocyanin concentration with the tube length. The finite difference method was used to solve the partial derivates. Were evaluated the effects of flow rate, solid content, heat exchange temperature, and tube length and diameter ratio. Our finds indicated that even considering the critical processing conditions, the losses of anthocyanins do not reach 1%, confirming its high thermal stability.

Keywords Thermal processing · Fruit pulp · Pigments · UV–visible spectroscopy · Thermodynamic analysis

List of symbols

A	Absorbance
C_A	Anthocyanin concentration
C_{A0}	Initial anthocyanin concentration
C_p	Specific heat
D	Cylinder diameter
DF	Dilution factor
E	Activation energy
k	Kinetic rate constant
k_0	Pre-exponential constant of Arrhenius equation
k_T	Thermal conductivity
L	Cuvette optical path length (in Eq. 2)
L	Cylinder length (in Scheme 1)
S	Solid content (%)
R	Tube radius
T	Temperature (°C)
$t_{1/2}$	Half-life time
T_∞	Heat exchanger temperature
U	Global heat transfer coefficient
ε	Molar absorptivity
ρ	Density

1 Introduction

The açaí palm tree (*Euterpe precatoria* Mart.) is a native tree of the Amazon rainforest. Brazil is the main producer, consumer, and exporter of açaí [3]. Açaí fruits have received attention from the food and pharmaceutical market in recent decades due to their high energy and nutritional value. From these fruits, the açaí pulp is obtained, being a product with high energy value, nutritive potential, high fiber, protein, and lipid content [7]. Açaí has an intense purple color; thus, it has been used

✉ Luís Marangoni Júnior, marangoni.junior@hotmail.com | [1]Department of Food Technology, School of Food Engineering, University of Campinas, Rua Monteiro Lobato, 80 – Cidade Universitária Zeferino Vaz, Campinas, SP CEP 13083-862, Brazil. [2]Department of Bioprocesses and Materials Engineering, School of Chemical Engineering, University of Campinas, Campinas, SP, Brazil.

in the production of natural dyes. It has drawn attention to the food market as ordinary artificial dyes tend to be replaced by natural ones [6].

Among the bioactive compounds present in açaí, flavonoids such as anthocyanins stand out (cyanidin-3-glucoside and cyanidin-3-rutinoside) [13]. Anthocyanin pigments are of prominent importance in fruits because of their dual role; first, they are an integral part of sensory attributes, and second, they have several biological properties [12]. Anthocyanins are present in many vegetables, giving colors and shades of red, blue, and purple, whose intensity is a function of the compound concentration [5]. The presence of these substances is mainly linked to antioxidant, anti-inflammatory, antiproliferative, and cardioprotective activities [13]. Due to its properties, açaí has received considerable attention in recent years as a new "super fruit" [11].

This fruit can be eaten fresh; however, the commercialization of raw fruit can lead to rapid degradation due to its high perishability [9]. Therefore, processing is a promising alternative. Among the processed foods that contain açaí berry and released on the world market in the last 5 years, 22% are juices, 12% energy and sports drinks, 9% snacks, 7% desserts and ice cream, 5% dairy category, and 3% sweets and candies, with the United States (30%), Brazil (19%), and Canada (8%) being the most representative countries in the launch of these products in recent years [2].

However, the processing of açaí can lead to anthocyanin degradation and consequently loss of color in the products. Heat treatment is one of the most commonly used food preservation methods to extend shelf life and ensure safety [19, 24]. However, the stability of anthocyanins is influenced by several factors, such as the food physical–chemical properties, the processing, and storage conditions [16]. Processing time and temperature are the most important factors affecting the stability of anthocyanin in food processing, where these conditions will be determined according to product characteristics and intended shelf life [18, 19]. Also, in this context, during industrial processing it is necessary to continuously monitor pigment degradation, since pigment degradation may reflect changes in sensory and nutritional aspects of products.

Food degradation kinetics is a complex phenomenon. However, empirical mathematical modeling techniques can be used to determine the kinetic effect. Kinetic parameters (reaction order, rate constant, and activation energy) provide useful information about changes that occur during thermal processing [25]. Thus, kinetic parameters determination and evaluation of anthocyanin thermal degradation become essential to predict the thermal processing conditions that will cause less degradation of açaí pulp anthocyanins.

Therefore, the aim of this study was to investigate the effect of processing time and temperature on the thermal degradation of anthocyanins, as well as to simulate the degradation in a tubular pasteurizer, considering the transient regime and thermal properties of açaí pulp.

2 Materials and methods

2.1 Pulp açaí

The açaí pulp was purchased at the Campinas Supply Center (CEASA) in the city of Campinas, SP, Brazil. The product was kept frozen at − 18 °C before analysis. According to the manufacturer's information, labeled on the packaging, the açaí pulp has 6.2 g of carbohydrates, 0.8 g of protein, 3.9 g of total fat, and 2.6 g of dietary fiber (13.5 g of solids in the 100 g portion). The pulp was composed only by açaí berry and water, which is necessarily added during the pulp extracting processing.

2.2 Sample preparation and thermal processing

Açaí pulp was thawed overnight at 5 °C before thermal processing. 15 mL of pulp was added into 1-cm-diameter screw-cap glass tubes to ensure isothermal heating and minimize atmospheric oxidation. Thermal degradation was performed at 60, 70, 80, and 90 °C in an ultra-thermostated bath (MA184, Marconi). The processes were monitored for 90 min, and an aliquot of the sample was collected at times 0, 5, 10, 20, 30, 60, and 90 min for each temperature analyzed. The tubes were immediately cooled in an ice bath and then stored at 5 °C until analysis.

2.3 Determination of monomeric anthocyanin content

Monomeric anthocyanin concentration of the samples was analyzed by UV–Visible spectroscopy (DU730, Beckman Coulter) using the differential pH method [15]. The samples were centrifuged (Avanti J-26 XPI, Beckman Coulter) at 4000 g for 10 min at 5 °C, and then, two sample dilutions were prepared using the supernatant: pH 1.0 buffer and pH 4.5 buffer. The sample absorbance was calculated using Eq. 1.

$$A = \left(A_{520} - A_{700}\right)\ \text{pH} = 1.0 - \left(A_{520} - A_{700}\right)\ \text{pH} = 4.5 \quad (1)$$

where A_{520} is the absorbance at wavelength 520 nm, and A_{700} is the absorbance at wavelength 700 nm. The

monomeric anthocyanin content of the sample was calculated using Eq. 2.

$$C_A = \frac{A \times MW \times DF \times 1000}{\varepsilon \times L} \quad (2)$$

where C_A is the concentration of anthocyanin (mg L^{-1}), MW is the molecular weight of monomeric anthocyanin (449.2 g mol^{-1}), DF is the dilution factor (30), ε is the molar absorptivity (26,900 L mol^{-1} cm^{-1}), and L is the length of the bucket path (1 cm).

2.4 Kinetic modeling

At a constant temperature, the anthocyanin thermal degradation kinetics was described as a first-order reaction. Equation 3 presents its integrated form.

$$\frac{C_A}{C_{A0}} = e^{-kt} \quad (3)$$

where C_A is the total anthocyanin concentration experimentally determined at time "t", and C_{A0} is the anthocyanin measured at zero time. For such reactions, temperature effects on the thermal degradation rate constant "k" may be expressed with an Arrhenius equation (Eq. 4).

$$k = k_0 e^{-E/RT} \quad (4)$$

where k_0 is the pre-exponential factor, E is the activation energy for the process degradation (J mol^{-1}), R is the gas constant (J mol^{-1} K^{-1}), and T is the process temperature (K). In addition, $t_{1/2}$ was calculated by ln2/k.

2.5 Thermodynamic analysis

The activation enthalpy (ΔH), the free energy of inactivation (ΔG), and the entropy (ΔS) were calculated using Eqs. 5–7 [17].

$$\Delta H = E - R \times T \quad (5)$$

$$\Delta G = -R \times T \times ln\left(\frac{k \times h}{k_B \times T}\right) \quad (6)$$

$$\Delta S = \frac{\Delta H - \Delta G}{T} \quad (7)$$

where E is the activation energy for the anthocyanin thermal degradation (J mol^{-1}), R is the ideal gas constant (8.314 J mol^{-1} K^{-1}), T is the temperature (K), k is the kinetic rate constant (s^{-1}), k_B is the Boltzmann constant (1.3806×10^{-23} J K^{-1}), and h is Planck's constant (6.6262×10^{-34} J s).

2.6 Mathematical modeling for a tubular reaction system

In this work, it was considered a tubular reactor with a jacket for heat transfer (Scheme 1), and operating parameters are shown in Table 1. The mass balance took into consideration a transient regime and also variation of anthocyanin concentration with the tube length. Equation 8 provides the mass balance for the situation analyzed in this work.

$$\frac{\partial C_A}{\partial t} = -\frac{v}{\pi R^2}\frac{\partial C_A}{\partial x} - kC_A \quad (8)$$

where the term $\frac{v}{\pi R^2}\frac{\partial C_A}{\partial x}$ stands for the anthocyanin concentration changes through the tube length, and kC_A stands for the kinetics of anthocyanin thermal degradation.

The energy balance for the tubular reactor represented by Scheme 1 is expressed by Eq. 9. In this case, it was also considered thermal diffusion through the reactor length.

$$\frac{\partial T}{\partial t} = \frac{k_T}{\rho C_p}\frac{\partial^2 T}{\partial x^2} - \frac{v}{\pi R^2}\frac{\partial T}{\partial x} + \frac{2U}{\rho C_p R}\left(T_\infty - T\right) \quad (9)$$

where the term $\frac{k_T}{\rho C_p}\frac{\partial^2 T}{\partial x^2}$ stands for the heat transfer by diffusion through the tube, the term $\frac{v}{\pi R^2}\frac{\partial T}{\partial x}$ stands for the thermal energy changes in the infinitesimal element via fluid input and output, and the term $\frac{2U}{\rho C_p R}\left(T_\infty - T\right)$ stands for the thermal energy transition through the reactor walls. The fundamental dynamic equations present initial and boundary conditions:

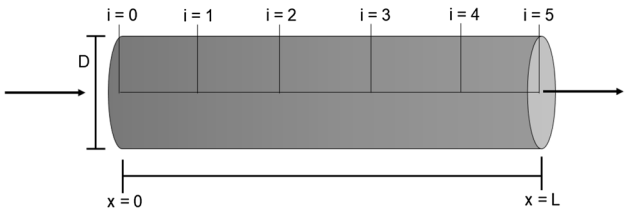

Scheme 1 Tubular reactor considered in this work

Table 1 Operating parameters used in the simulations

Parameters	Value	Unit
L/D ratio	1000	[ ]
Flow rate, v	5.28×10^{-5}	$m^3\ s^{-1}$
Anthocyanin concentration, C_{A0}	340	mg L^{-1}
Inlet temperature, T_0	25	°C
Heating fluid temperature, T_∞	70	°C
Total solid content, S	10	%
Global coefficient of heat exchange, U	400	J s^{-1} m^{-2} K^{-1}

At $t=0$; $C_A=C_{A0}$ and $T=T_0$ (it was considered that at in initial stages, the concentration of anthocyanin through the tube is equal to the entrance. The same was considered for the temperature). At $t>0$; for $x=0$; $C_A=C_{A0}$ and $T=T_0$. For $x=L$; $C_A=C_A$ and $T=T$.

The backward finite differences were used to replace the partial derivates related to the length, and the forward finite differences were used to replace the partial derivative related to time, resulting in the system of algebraic difference equations for the dependent variables at each grid point (Eqs. 10 and 11). The grid points were defined by the equidistant division of the interval [0, L] on "n" subintervals of length $\Delta x=L/5$ (scheme 1), and Δt, which was small enough to satisfy the stability condition in each simulation.

$$\frac{C_{Ai,j+1}-C_{Ai,j}}{\Delta t}=-\frac{v}{\pi R^2}\left[\frac{C_{Ai,j}-C_{Ai,j-1}}{\Delta x}\right]-kC_{Ai,j} \quad (10)$$

$$\frac{T_{i,j+1}-T_{i,j}}{\Delta t}=\frac{k_T}{\rho C_p}\left[\frac{T_{i,j}-2T_{i-1,j}+T_{i-2,j}}{(\Delta x)^2}\right]-\frac{v}{\pi R^2}\left[\frac{T_{i,j}-T_{i-1,j}}{\Delta x}\right]+\frac{2U}{\rho C_p R}\left(T_\infty-T_{i,j}\right) \quad (11)$$

Table 2 provides the physical–chemical parameters used to simulate the process. Regarding açaí physical properties, it was reported in the literature that density, specific heat, thermal conductivity, and thermal diffusivity are mainly affected by the solid content and temperature [6]. Therefore, in this present study the simulations were evaluated according to the solid content (S) in order to verify how much its value affects the anthocyanin losses. In addition, simulations were also carried out considering the effect of reactor length and diameter ratio (L/D), volumetric flow rate (v), and heat exchanger temperature (T_∞).

3 Results and discussion

3.1 Kinetic model fitting

Figure 1a shows the experimental results of anthocyanin thermal degradation in açaí pulp as a function of time, with adjustment of a 1st-order reaction kinetic model (parameters shown in Table 3). The onset of the degradation process occurs slightly more intensely for all temperatures. Despite this, there is an exponential reduction of C_A,

Table 2 Physical–chemical parameters used to simulate the tubular reaction system during transient regime

Physical properties	Parameters	Value/expression	Unit	References
Kinetic rate constant	k	$k=36.6\times e^{-42800/RT}$	s^{-1}	This work
Thermal conductivity	k_T	$k_T(S,T)=0.4398+7.1277\times10^{-3}(S)+2.5385\times10^{-3}(T)-6.959\times10^{-5}(S)(T)-2.6173\times10^{-4}(S)^2$	W m^{-1} K^{-1}	[6]
Specific heat	C_p	$C_p(S,T)=4.381-3.8413\times10^{-2}(S)-5.28\times10^{-4}(T)+1.4933\times10^{-4}(S)(T)$	J kg^{-1} K^{-1}	[6]
Density	ρ	$\rho(S,T)=1014.509-0.3185(S)-0.1280(T)-0.0083(S)(T)+0.0994(S)^2-0.0025(T)^2$	kg m^{-3}	[6]

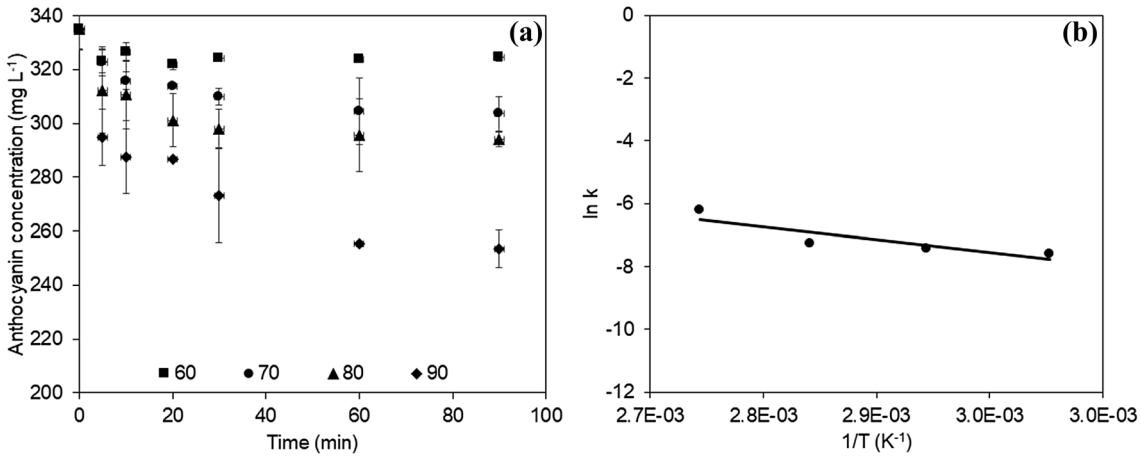

Fig. 1 **a**Reduction in anthocyanin concentration as a function of time for 60, 70, 80, and 90 °C, and **b** kinetic rate constant natural logarithm as a function of the reciprocal temperature

Table 3 First-order kinetic models adjusted for each temperature

Temperature (°C)	Adjusted equation	Rate constant (min^{-1})	R^2	$t_{1/2}$ (h)
60	$C_A = 334.9e^{-0.0005 \times t}$	0.0005	0.7504	23
70	$C_A = 334.9e^{-0.0006 \times t}$	0.0006	0.8131	19
80	$C_A = 334.9e^{-0.0007 \times t}$	0.0007	0.8205	16
90	$C_A = 334.9e^{-0.002 \times t}$	0.002	0.8406	7

Table 4 Variation of enthalpy, free energy, and entropy for the thermal degradation process of anthocyanins in açaí pulps

T (°C)	ΔH (kJ mol^{-1})	ΔG (kJ mol^{-1})	ΔS (kJ mol^{-1} K^{-1})
60	40.049	114.240	−222.797
70	39.965	117.235	−225.276
80	39.882	120.285	−227.770
90	39.799	120.608	−222.615

and a good fit for the experimental data set as a whole, indicating that this model can be used to reproduce the process by simulation. Anthocyanin content in açaí pulp decreased as temperature and heating time increased, as reported in the literature for other fruit processing [4, 19, 21, 22]. Figure 1b provides the natural logarithm of the rate constant as a function of the reciprocal temperature to identify Arrhenius' parameters, which are the pre-exponential factor (k_0) and activation energy (E_a).

Table 3 provides four kinetic models adjusted to the experimental degradation data for each temperature evaluated in Fig. 1a. In each model, the pre-exponential factor (C_{A0}) was defined as the constant value of 334.9 mg L^{-1}, which refers to the total anthocyanin concentration at time zero. In addition, the rate constant (k) exponentially varies as the temperature increases. The $t_{1/2}$ values are also presented in Table 3.

By fitting a straight line, the Arrhenius parameters were determined as follows: $k_0 = 2.2 \times 10^3$ min^{-1} and $E = 42.8$ kJ mol^{-1}, with determination coefficient (R^2) equals to 0.8. Activation energies for anthocyanin degradation during heating have dispersed values in the literature: 68.04 kJ mol^{-1} for acerola [21], 99.7 kJ mol^{-1} for jussara grapes [19], 80.4 kJ mol^{-1} for blueberry juice [14], and 24.16 kJ mol^{-1} for açaí pulp [6]. The result of this work is between the reported values, but different from the value found by Costa et al. [6]. Despite this difference of just over 40%, it appears that the anthocyanins of the açaí pulp follow a pattern: They are less sensitive to temperature variation than those found in other fruits, since lower activation energies besides indicating an energetic barrier to the reaction occurrence, it suggests greater stability to the temperature variation.

3.2 Thermodynamic analysis

Table 4 shows the calculated results of activation enthalpy (Eq. 5), free energy (Eq. 6), and entropy (Eq. 7) for anthocyanin thermal degradation at each temperature. The positive ΔH value represents an endothermic state for the process. The observed decrease in ΔH with increasing temperature indicates that the energy barrier required for bond breakage is slightly lower at higher temperatures, indicating slightly higher degradation rates with increasing temperature. The free energy variation, ΔG, describes the spontaneity of the process by the difference between the activated state and the reactant state. Positive values of ΔG were observed for all temperatures used in the processing of açaí pulp, showing that anthocyanin degradation is not spontaneous.

It is known that when the activation entropy (ΔS) values are high, generally positive, the system is away from the thermodynamic equilibrium, and consequently, the system tends to generate a faster activated complex due to the higher reactivity [10]. In contrast, negative values of ΔS indicate that molecules in the transition state are more organized than those at the beginning of the reaction, providing lower reactivity. For all temperatures analyzed in this work, the values of ΔS had negative values, justifying the low degradation rate illustrated in Fig. 1a.

3.3 Transient process simulations

Computational simulations were performed by numerical resolution of Eqs. 8 and 9, aiming to evaluate the anthocyanin losses during the pasteurization process of açaí pulps in a tubular system. The mathematical model resolution allowed to predict the anthocyanin concentration and pasteurizer temperature profiles as a function of time and length. Differently from what was presented in this work, the models described in the literature were developed for ideal simple piston flow [21, 23], canned food pasteurization systems [20], and tunnels pasteurization [8], in addition to traditional plate pasteurization systems [1].

Figure 2 shows the reaction system divided into 5 grid points, from $i = 0$ (system input) to $i = 5$ (system output), with (a) the anthocyanin concentration profile and (b) the temperature profile. Table 1 presents the operational parameters considered in this simulation. Figure 2a shows an exponential decay of anthocyanin concentration as a function of time, reaching a constant value (steady state) as expected for this system. Through this figure, it is

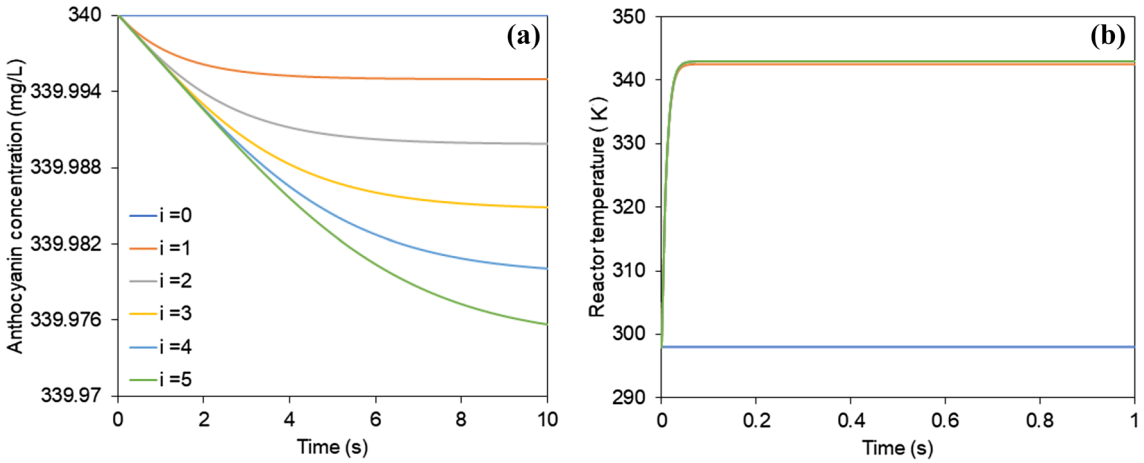

Fig. 2 **a** Reduction in anthocyanin concentration as a function of time at three reactor points, where $i=0$ is equivalent to system input and $i=5$ is equivalent to system output and **b** reactor temperature as a function of time

possible to predict the exact time for the system to reach the steady state, in which the loss of anthocyanin, quantified at the output, will be kept constant. It is also verified that the concentration at the system exit ($i=5$) is practically the input value, reaffirming the good thermal stability of anthocyanins in açai pulps, evaluated by their kinetic parameters determined in Sect. 3.1.

Figure 2b shows the internal temperature profile of the reaction system keeping the temperature of the jacket fixed and at its maximum value (thermal losses were disregarded). Note that the reaction system rapidly reaches the heating fluid temperature (< 1 s). This is a critical situation that would hardly occur in practice, since the heat exchanger temperature presents a longitudinal temperature gradient, causing the internal temperature to reach lower values. In addition, radial temperature gradients were also neglected in this work, since high L/D ratio was considered. This work simulated the process under these critical conditions, which would be the worst possible to obtain the maximum losses of anthocyanins.

Figure 3 illustrates the effect of the most common process operating parameters on the anthocyanin concentration profile at system output. In these simulations, the parameters of Table 1 were kept constant, with changes in some key parameters. Figure 3a, for example, illustrates the effect on system flow rate, where it is found that lower flow rates provide higher degradation rates. The minimum flow considered in this figure is also considered a critical situation, since in general, the systems operate with higher flow rates, indicating that the anthocyanins will still present a low degradation percentage.

Figure 3b indicates that during industrial processing, the percentage of total solids in the açaí pulp does not influence its anthocyanin degradation. Costa et al. [6] demonstrated that this percentage has effects on the pulp thermal properties (Table 2). However, its effect on the temperature profile is quite low and therefore negligible in the anthocyanin degradation. Figure 3c shows the effect of the heat exchange temperature, and as expected, the higher its value, the higher the degradation rate. Finally, Fig. 3d illustrates that increasing the pipe length-to-diameter ratio (L/D) causes an increase in the degradation rate. Even so, for these last two cases, considering the upper limit values ($T_\infty = 100$ °C and $L/D = 3000$), the loss of anthocyanin does not reach 1%, allowing to infer that this microconstituent presents an optimal thermal stability in the açaí pulp.

4 Conclusions

In this work, kinetic and thermodynamic parameters were successfully determined for anthocyanin thermal degradation. The kinetic model fitted followed a first order, with activation energy equals to 42.8 kJ mol^{-1}. This value is considered low, and it can be concluded that for a large anthocyanin degradation rate, a large temperature variation is required. To support this first conclusion, a thermodynamic analysis was performed, along with thermal processing simulations in a tubular system, in which different operational parameters were evaluated.

The observed decrease in ΔH with the increase in temperature indicated slightly higher degradation rates with increasing temperature. Positive values of ΔG were observed for all temperatures used in the processing of açaí pulp, showing that anthocyanin degradation is not spontaneous. Moreover, for all temperatures analyzed in this work, the values of ΔS had negative values, corroborating what was indicated in the estimation of the kinetic parameters.

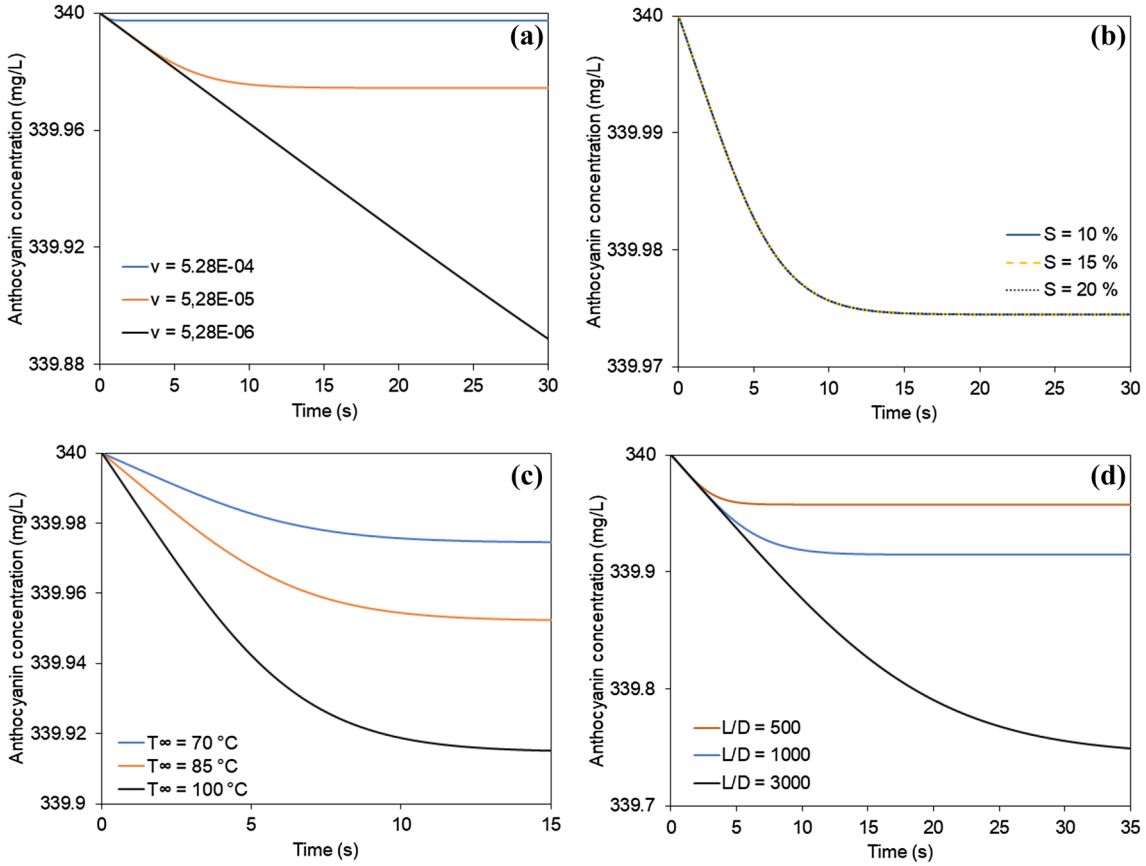

Fig. 3 Effect of operating parameters on the concentration of anthocyanins at the outlet of the tubular pasteurizer: **a** effect of flow, **b** effect of total solid content on açai pulp, **c** temperature effect of heat exchange fluid, and **d** effect of pasteurizer length-to-diameter ratio (*L*/*D*)

The effect on system flow rate showed that lower flow rates provide higher degradation rates. It was also found that the percentage of total solids in the açaí pulp does not influence its anthocyanin degradation. The effect of the heat exchange temperature showed that the higher its value, the higher the degradation rate. Finally, increasing the *L*/*D* ratio causes an increase in the degradation rate. Even so, for all cases, considering the critical limit values, the losses of anthocyanins do not reach 1%. It can be concluded that this microconstituent has high thermal stability even under critical processing conditions.

Acknowledgements The authors thank the ao Conselho de Desenvolvimento Científico e Tecnológico (CNPq) for the granted PhD and scientific initiation scholarship. This study was funded in part by the *Coordenação de Aperfeiçoamento de Pessoal Nível Superior—Brasil (CAPES)*—Financial Code 001.

Compliance with ethical standards

Conflict of interest The authors declare that they have no conflict of interest.

References

1. Aguiar HF, Gut JAW (2014) Continuous HTST pasteurization of liquid foods with plate heat exchangers: mathematical modeling and experimental validation using a time-temperature integrator. J Food Eng 123:78–86. https://doi.org/10.1016/j.jfoodeng.2013.09.022
2. Bezerra VS (2016) Açaí : produção de frutos, mercado e consumo, 19
3. Boeira LS, Freitas PH, Uchoa NR, Bezerra JA, Cád SV, Junior SD, Albuquerque PM, Mar JM, Ramos AS, Machado MB, Maciel LR (2020) Chemical and sensorial characterization of a novel alcoholic beverage produced with native açaí (Euterpe precatoria)

from different regions of the Amazonas state. LWT Food Sci Technol 117:108632. https://doi.org/10.1016/j.lwt.2019.108632
4. Buvé C, Kebede BT, De Batselier C, Carrillo C, Pham HT, Hendrickx M, Grauwet T, Van Loey A (2018) Kinetics of colour changes in pasteurised strawberry juice during storage. J Food Eng 216:42–51. https://doi.org/10.1016/j.jfoodeng.2017.08.002
5. Cavalcanti RN, Santos DT, Meireles MAA (2011) Non-thermal stabilization mechanisms of anthocyanins in model and food systems: an overview. FRIN 44(2):499–509. https://doi.org/10.1016/j.foodres.2010.12.007
6. Costa HCB, Silva DO, Gustavo L, Vieira M (2018) Physical properties of açai-berry pulp and kinetics study of its anthocyanin thermal degradation. J Food Eng 239:104–113. https://doi.org/10.1016/j.jfoodeng.2018.07.007
7. Costa RG, Andreola K, Mattietto RDA, de Faria LJ, Taranto OP (2015) Effect of operating conditions on the yield and quality of açai (Euterpe oleracea Mart.) powder produced in spouted bed. LWT Food Sci Technol 64:1196–1203. https://doi.org/10.1016/j.lwt.2015.07.027
8. Dilay E, Vargas JVC, Amico SC, Ordonez JC (2006) Modeling, simulation and optimization of a beer pasteurization tunnel. J Food Eng 77(3):500–513. https://doi.org/10.1016/j.jfoodeng.2005.07.001
9. Franco B, Carlos R, Alberto J, Costa V (2018) Biocompounds and physical properties of açaí pulp dried by different methods. LWT Food Sci Technol 98(June):335–340. https://doi.org/10.1016/j.lwt.2018.08.058
10. Georgieva V, Zvezdova D, Vlaev L (2012) Non-isothermal kinetics of thermal degradation of chitosan. Chem Cent J 6(1):1–10. https://doi.org/10.1186/1752-153X-6-81
11. Kang J, Thakali KM, Xie C, Kondo M, Tong Y, Ou B, Jensen G, Medina MB, Schauss AG, Wu X (2012) Bioactivities of açaí (Euterpe precatoria Mart.) fruit pulp, superior antioxidant and anti-inflammatory properties to Euterpe oleracea Mart. Food Chem 133(3):671–677. https://doi.org/10.1016/j.foodchem.2012.01.048
12. Kara S, Erçelebi EA (2013) Thermal degradation kinetics of anthocyanins and visual colour of Urmu mulberry (*Morus nigra* L.). J Food Eng 116:541–547. https://doi.org/10.1016/j.jfoodeng.2012.12.030
13. Kazumy K, Yamaguchi DL, Felipe L, Pereira R, Victor C, Silva E, Florêncio V (2015) Amazon açaí: chemistry and biological activities: a review. Food Chem 179:137–151. https://doi.org/10.1016/j.foodchem.2015.01.055
14. Kechinski CP, Guimarães PVR, Noreña CPZ, Tessaro IC, Marczak LDF (2010) Degradation kinetics of anthocyanin in blueberry juice during thermal treatment. J Food Sci 75(2):173–176. https://doi.org/10.1111/j.1750-3841.2009.01479.x
15. Lee J, Durst RW, Wrolstad RE (2005) Determination of total monomeric anthocyanin pigment content of fruit juices, beverages, natural colorants, and wines by the pH differential method: collaborative study. J AOAC Int 88:1269–1278
16. Martynenko A, Chen Y (2016) Degradation kinetics of total anthocyanins and formation of polymeric color in blueberry hydrothermodynamic (HTD) processing. J Food Eng 171:44–51. https://doi.org/10.1016/j.jfoodeng.2015.10.008
17. Mercali GD, Jaeschke DP, Tessaro IC, Marczak LDF (2013) Degradation kinetics of anthocyanins in acerola pulp: comparison between ohmic and conventional heat treatment. Food Chem 136(2):853–857. https://doi.org/10.1016/j.foodchem.2012.08.024
18. Patras A, Brunton NP, O'Donnell C, Tiwari BK (2010) Effect of thermal processing on anthocyanin stability in foods; mechanisms and kinetics of degradation. Trends Food Sci Technol 21(1):3–11. https://doi.org/10.1016/j.tifs.2009.07.004
19. Peron DV, Fraga S, Antelo F (2017) Thermal degradation kinetics of anthocyanins extracted from juçara (Euterpe edulis Martius) and "Italia" grapes (*Vitis vinifera* L.), and the effect of heating on the antioxidant capacity. Food Chem 232:836–840. https://doi.org/10.1016/j.foodchem.2017.04.088
20. Plazl I, Lakner M, Koloini T (2006) Modeling of temperature distributions in canned tomato based dip during industrial pasteurization. J Food Eng 75(3):400–406. https://doi.org/10.1016/j.jfoodeng.2005.04.057
21. Silva NL, Crispim JMS, Vieira RP (2017) Kinetic and thermodynamic analysis of anthocyanin thermal degradation in acerola (Malpighia emarginata D.C.) pulp. J Food Process Preserv 41(4):1–7. https://doi.org/10.1111/jfpp.13053
22. Sinela A, Rawat N, Mertz C, Achir N, Fulcrand H, Dornier M (2017) Anthocyanins degradation during storage of *Hibiscus sabdariffa* extract and evolution of its degradation products. Food Chem 214:234–241. https://doi.org/10.1016/j.foodchem.2016.07.071
23. Vieira RP, Mokochinski JB, Sawaya ACHF (2015) Mathematical modeling of the ascorbic acid thermal degradation in orange juice during industrial pasteurizations. J Food Process Eng. https://doi.org/10.1111/jfpe.12260 **(in press)**
24. Wang W, Xu S (2007) Degradation kinetics of anthocyanins in blackberry juice and concentrate. J Food Eng 82:271–275. https://doi.org/10.1016/j.jfoodeng.2007.01.018
25. Yang Z, Han Y, Gu Z, Fan G, Chen Z (2008) Thermal degradation kinetics of aqueous anthocyanins and visual color of purple corn (Zea mays L.) cob. Innov Food Sci Emerg Technol 9:341–347. https://doi.org/10.1016/j.ifset.2007.09.001